

Prototype Studies for the CLEO III RICH

RICH Note No. 3

S. Kopp, M. Artuso, A. Efimov, M. Gao, S. Playfer, R. Mountain, F. Muheim and S. Stone
Department of Physics, Syracuse University, Syracuse NY 13244, USA

Abstract

We describe a prototype RICH detector that has been built as part of design work for the CLEO III RICH. Cherenkov photons are produced in a LiF radiator, and are detected in a multiwire chamber with a CaF_2 entrance window containing a gas mixture of methane and TEA. Signals are read out from 2016 cathode pads using low noise Viking chips. First results from this prototype show a yield of 13 photoelectrons per image in agreement with our design studies.

I. DESCRIPTION OF PROTOTYPE RICH

As part of the upgrade of the CLEO experiment to CLEO III, a Ring Imaging Cherenkov detector will be installed to provide good particle identification. The design of this detector is described in the contribution by M. Artuso [1] to these proceedings.

To test our understanding of the design parameters of the RICH, and to gain experience in the construction of such a system, we have built a prototype detector. The radiator is a plane LiF crystal 1cm thick, and $6\text{cm} \times 6\text{cm}$ in area. Photons produced in this radiator pass through an expansion gap of 15.7cm filled with pure nitrogen, and are detected in a multiwire chamber filled with a photosensitive gas mixture produced by bubbling methane through liquid Triethylamine (TEA) at 15°C . The photon detector has a sensitive area of $82.5\text{cm} \times 13.7\text{cm}$ corresponding to one third of the length of a full detector module in the CLEO III design. This area is sufficient to contain 90% of the Cherenkov photons from a track passing through the centre of the radiator at an angle of incidence of 30° .

Figure 1 shows the design of the photon detector. There is a UV transparent CaF_2 entrance window made by gluing together six CaF_2 crystals end-to-end with Torrseal [2]. This window is mounted in an aluminium frame using a plastic hinge to mechanically decouple the crystals from the rest of the detector. Field-shaping strips $100\mu\text{m}$ wide are evaporated onto the crystals across the width of the detector at 2.5mm intervals. The photons convert in the chamber with a mean free path of 0.5mm, and the photoelectrons drift to a plane of $20\mu\text{m}$ anode wires strung along the length of the detector. At the anode wires gas amplification occurs, and the signals induced on a plane of 2016 cathode pads $7.5\text{mm} \times 7.5\text{mm}$ are used to measure the position of the photon. Ceramic spacers at 28cm intervals

maintain the 1mm spacing between the anode and cathode planes.

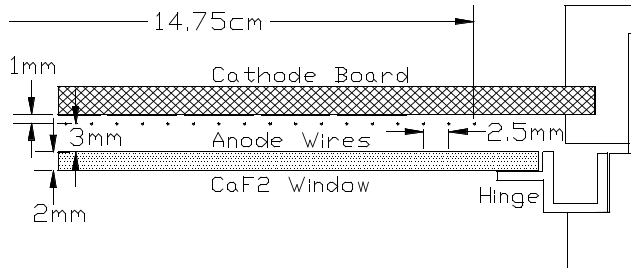


Figure 1: Geometry of the Photon Detector.

The quantum efficiency of methane+TEA is limited to wavelengths between 135nm and 165nm [4], so good transmission is required from the radiator to the photon detector in this range. We have used a UV monochromator to measure the effective transmissions at 150nm. The LiF radiator and the CaF_2 window have transmissions of 83% and 80% respectively. The transparency of the N_2 in the expansion volume is 96% if the flow rate is sufficient to change one volume per hour.

II. READOUT ELECTRONICS

We believe it is important for the stability of operation of a large system to run at a moderate gain of a few 10^4 . At this gain the pulse height distribution from single photoelectrons is exponential, so a low noise threshold is needed to achieve high efficiency[3]. We are using the Viking VA2 chip [5], which has been developed for reading out solid state detectors. Each chip has 128 channels of amplifier/shaper with a $1\mu\text{s}$ peaking time, and an intrinsic noise performance of 200 electrons. We use 63/128 channels on each chip to read out the cathode pads. The 32 chips are mounted on ceramic chip carriers, which in turn are mounted on readout boards. The readout boards are daisy-chained into four repeater cards that further amplify the signals, and send them to a 10-bit ADC for digitization. We received two batches of Viking chips with gains of 35mV/fC and 70mV/fC, but equalized out the gains in the repeater cards so that one ADC count always corresponds to 178 electrons.

The noise level of the complete system is measured to be 400 electrons (FWHM). There is very little coherent noise, and the system has been stable for several months. The only problem has been the lack of input protection on the

Viking chips. As a consequence of sparking during chamber operation, one chip is dead and another has become very noisy. A custom Viking chip is being built for use by us in CLEO III which will have input protection on each channel [1].

III. RESULTS

The prototype has been operated in a cosmic ray stand with two different types of triggers (see Figure 2). If we trigger on charged tracks passing through the radiator at an angle of incidence of 30° , we observe the ring image in the detector, but not the charged track itself, due to the small width of the detector. Alternatively we can trigger on charged tracks that pass through the photon detector, in which case we do not observe the photons in the ring image (two possible variations exist on this last option: in the first, the track passes through the N_2 volume directly into the photon detector; in the second, the track passes through a second piece of LiF located over the chamber and then through the chamber itself—see Figure 2). At present the cosmic ray stand does not have any tracking chambers, so the track parameters at the radiator are not known.

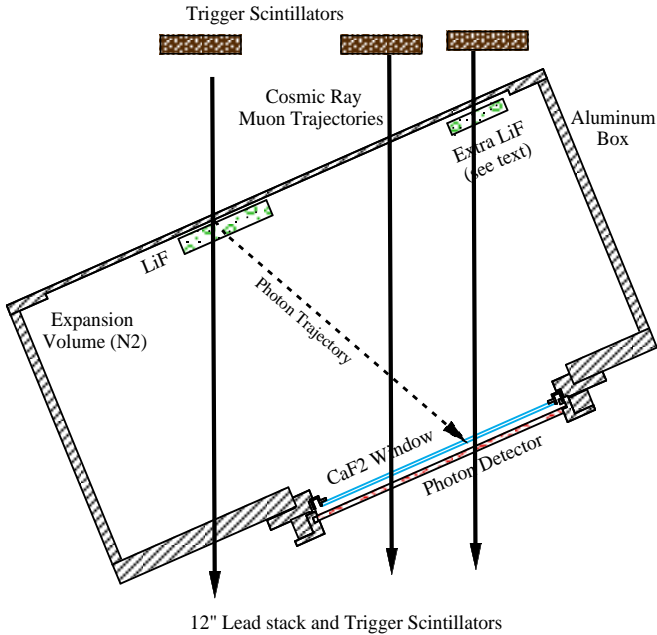


Figure 2: Set-up for the Syracuse cosmic ray test stand. Scintillator paddles trigger on cosmic ray particles, and extra paddles above the RICH prototype are used to veto against multi-particle showers. A 12 in. lead stack below the RICH provides a momentum cut of $1 \text{ GeV}/c$ in the trigger.

Figures 3(a) and (b) show examples of events in which we detect the ring image. Clusters of pads corresponding to single photoelectrons can be seen. The sum of many events (Figure 3(c)), shows the acceptance of our trigger,

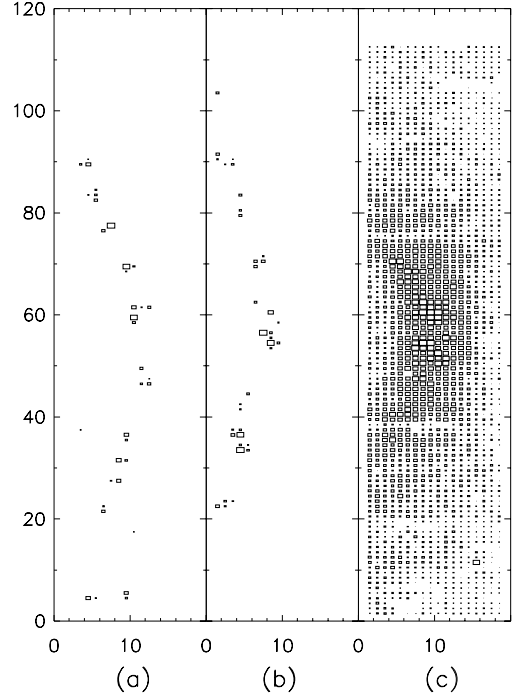


Figure 3: (a) and (b) Pad distributions for single ring image events, and (c) for the sum of many events

and the low level of background hits and electronic noise. The dead areas at rows 38, 57 and 76 are due to the joints in the CaF_2 window and the ceramic spacers between the anodes and cathode pads.

The typical operating point for the prototype is with the anodes at $+1500V$ and the window strips at $-1350V$. Figure 4 shows the charge distributions of the reconstructed single photoelectron clusters for several different anode voltages. The distributions are exponentials corresponding to gains in the 10^4 range. The noise level of 400 electrons is less than a tenth of the first bin. At these voltages the photoelectrons do not saturate the ADC, but the charged tracks do. We have been able to operate the chamber with the anodes at $+1700V$, when even the photoelectron clusters are in saturation.

We select ring image events that have at least one cluster, with a geometric distribution consistent with a track through the radiator. Since we do not have information on the track parameters, we are unable to distinguish clusters that belong to the image from noise and background clusters. To eliminate electronic noise we have made a very conservative cut at 5σ (about $900 e^-$). We have also removed 180 pad channels that are noisy (due to incidents of sparking), most of which are near the edges of the detector, and do not affect the acceptance significantly.

Figure 5 shows the number of photoelectrons observed in the detector as a function of the anode voltage. There is clear evidence of the onset of a plateau at about $1350V$. On the plateau there are 12.5–13 photoelectrons per event. If the noise cut is reduced to 3σ this number increases to

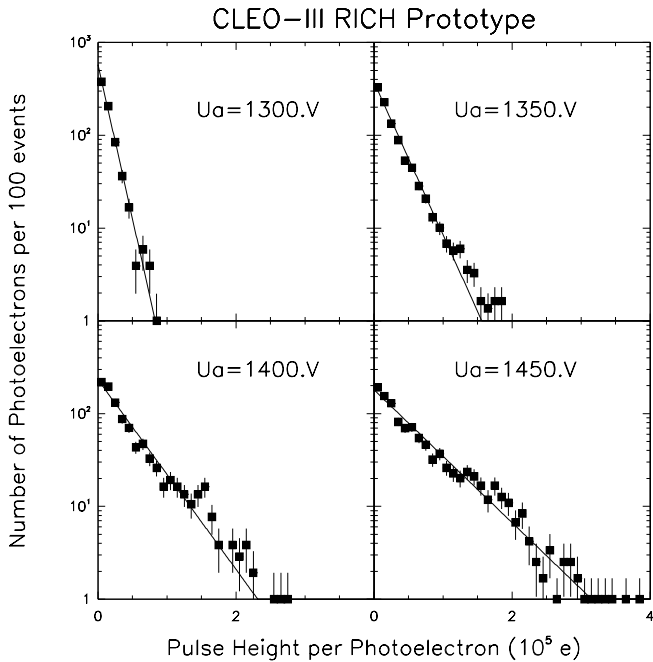


Figure 4: Photoelectron pulse height distributions at different anode voltages

13.5. There are a number of corrections in going from this number to the true number of photoelectrons per image. There are geometric acceptance losses due to the finite size of the detector, and due to the removal of the noisy pads. There are also losses of real photoelectrons and gains of fake photoelectrons due to the declustering algorithm used for separating overlapping photoelectron signals. These corrections have been studied with a Monte Carlo simulation. We find that the declustering algorithm leads to a net loss of about two photoelectrons. Our results correspond to a total of 15 photoelectrons per image after declustering, with 13.5 photoelectrons being inside the geometric acceptance of the detector.

The data with charged tracks passing through the detector have been used to study the effect of large signals on the electronics, and to study additional clusters in the detector. At the normal operating point of 1500 V, the saturated pulses from charged tracks give large cluster sizes of about ten pads. There is some contribution to this cluster size from Cherenkov photons and delta rays produced in the window. Away from the charged track we observe 0.7 additional clusters per event if the track passes through the additional LiF radiator located above the photon detector (see Figure 2), and 0.2 additional clusters if it does not. The clusters from the LiF have pulse heights consistent with single photoelectrons, and have a $1/r^2$ distribution about the charged track. Furthermore, if the expansion volume is not flushed with N_2 , the number of clusters falls from 0.7 to 0.2, even when the track passes through the extra radiator, indicating that these extra clusters are indeed due to photon emission of some sort in the radiator. This is consistent with incoherent photon production in the radiator as noted in [6]. We find that the observed yield and

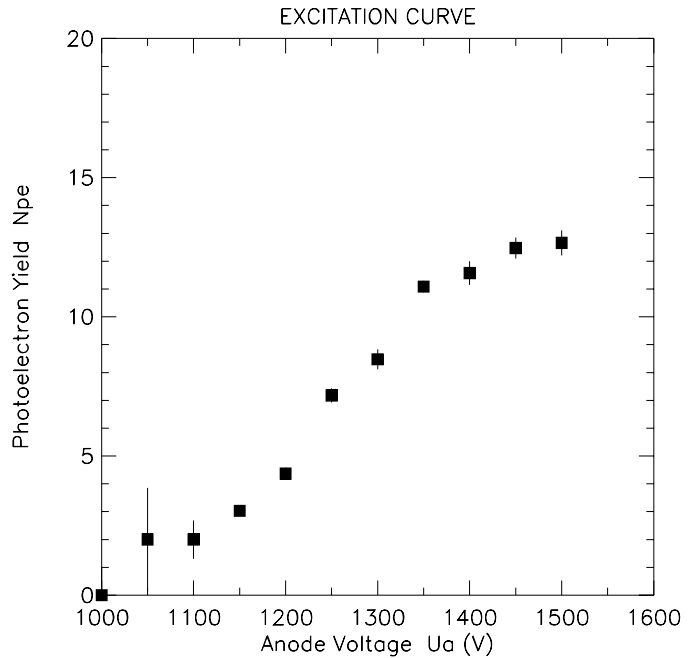


Figure 5: Plateau curve for methane+TEA.

$1/r^2$ distribution are consistent with the Cherenkov photons produced by delta rays in the LiF [7]. Extrapolating these additional clusters to the angular acceptance of the ring image data, we calculate a background of 0.5 to our Cherenkov signal due to this other source of photon production in the LiF. We have confirmed this estimate of 0.5 extra clusters by a visual scan of the ring image events.

IV. CONCLUSIONS

We have built and tested a prototype RICH detector with a LiF radiator and CH_4+TEA as the photosensitive gas. Using Viking VA2 chips to read out the 2016 cathode pads, we have achieved a very good noise performance of 400 electrons. The prototype has been operated at gains of a few 10^4 , where the photoelectron pulse height distributions are exponential. At these gains the detector is on plateau, indicating good efficiency. The observed yield is about 13 photoelectrons per image, in agreement with our Monte Carlo and background studies. These results convince us that a RICH detector can be successfully built for CLEO III.

V. ACKNOWLEDGEMENTS

We thank the National Science Foundation for support. We also thank Tom Ypsilantis and Jacques Séguinot for advising us on RICH detectors.

VI. REFERENCES

- [1] M. Artuso *et al.*, “The Ring Imaging Detector for CLEO III”, contribution to these proceedings.

- [2] The CaF_2 and LiF crystals are supplied by Optovac, North Brookfield, MA. Torrseal is supplied by Varian, Lexington, MA.
- [3] In our detector, the analog pulse height will be read out for each cathode pad. For an alternative to this view, where faster, digital electronics with simpler discriminator readout, a smaller cathode pad size, and a smaller anode-to-cathode separation are used, see the discussion of Ref. [4].
- [4] R. Arnold *et al.*, Nucl. Inst. and Meth. **A314** (1992) 465.
- [5] The Viking VA2 chip is produced by IDE AS, Oslo, Norway.
- [6] R. Arnold *et al.*, Nucl. Inst. and Meth. **A350** (1994) 430.
- [7] J.E.Grove and R.A.Mewaldt, Nucl. Inst. and Meth. **A314**, (1992) 495.